

MODERNIZATION AND OPERATION OF IONIZATION-PROPORTIONAL GAS COUNTER AT INR RAS PROTON LINAC

A. Melnikov[†], S. Gavrilov¹

Institute for Nuclear Research of the Russian Academy of Sciences, Troitsk, Moscow, Russia
¹also at Moscow Institute of Physics and Technology (National Research University), Moscow, Russia

Abstract

Multinode gas counter is used as a detector for low intensity proton beam diagnostics at INR RAS linac. The device consists of ionization chamber to measure beam current and two proportional chambers, based on stripe geometry, to measure beam profiles. The data is processed with Labview software. The models and methods predicting operational characteristics of the counter in ionization and proportional mode are presented. An analytical model of recombination was tested to predict the saturation voltage for ionization mode. Beam test results and operational characteristics of the counter are presented as well as results of investigations of counter degradation under the beam. A new design of a gas filled counter is also discussed.

INTRODUCTION

A proton irradiation facility (PIF) at INR RAS linac is used to study radiation effects in electronic components. This facility is characterized with operational parameters: proton energy - 20÷210 MeV; particles per pulse - $10^7 \div 10^{12}$; pulse duration - 0.3÷180 μ s; pulse repetition rate - 1÷50 Hz.

Partially diagnostics is realized with a beam current transformer (BCT) installed in the beam pipe. The BCT provides absolute nondestructive measurements of beam pulse current with the amplitude > 25 μ A. To measure beam current and profiles for less intensive beams MGC based on gas ionization is foreseen.

MULTIANODE GAS COUNTER

Multinode gas counter (MGC) [1] consists of 5 plates (Fig. 1) which are printed-circuit boards made of FR4 with 0.5 mm width. The metal covering is 18 μ m nickel, plated with 0.05 μ m immersive gold.

Three central plates form a dual gap ionization chamber. Electrons of primary ionization are collected at the middle anode plate by a quasi-uniform electrostatic field. This part of the detector allows to measure beam current in an ionization mode.

Lateral regions are proportional chambers for beam position and profile measurements. Electrons are collected at the multichannel anode structure, which consists of 25 stripes with 100 μ m width, 100 mm length and 4 mm spacing. Strong nonuniform field around stripes leads to electron avalanches, increasing the signal.

[†] alexei.a.melnikov@gmail.com

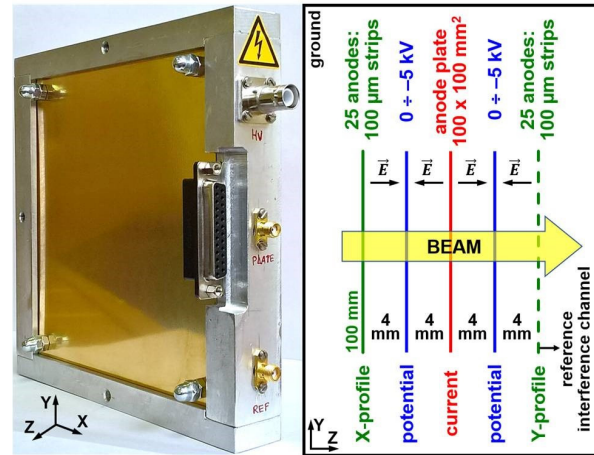


Figure 1: MGC photo and layout.

The total assembly of the counter is not sealed. The filling gas is atmospheric air.

The information about readout electronics and data acquisition system can be found elsewhere [2].

IONIZATION MODE

The number of primary ionization electrons defines the plateau level of ionization mode. The computed signal level based on dE/dx agrees with experimental results with 10% precision [2]. The gas composition was assumed as 80% N_2 and 20% O_2 molecules at standard conditions.

The measured signal from ionization chamber electrodes is caused by induced currents due to the moving electrons and ions: $i^{e,+,-}$ [3].

$$i^e(t) = \frac{Q_0}{t_{de}} \left(1 - \frac{t}{t_{de}}\right) \exp\left(-\frac{t}{T_a}\right).$$

$$i^+(t) = \frac{Q_0}{t_{d+}} \left(1 - \frac{t}{t_{d+}}\right).$$

$$i^-(t) = \frac{Q_0}{t_{d-}} \left[1 - \frac{t}{t_{d-}} - \frac{T_a}{t_{de}} \left\{1 - \exp\left(-\frac{t_{de}}{T_a} \left(1 - \frac{t}{t_{d-}}\right)\right)\right\}\right],$$

where Q_0 is the total charge of primary particles, $t_{de,+,-}$ is the drift time of electrons or ions of corresponding sign, T_a is an attachment time.

Content from this work may be used under the terms of the CC BY 3.0 licence (© 2020). Any distribution of this work must maintain attribution to the author(s), title of the work, publisher, and DOI

Electrons are involved in two- or three-body attachment reactions with O₂ molecules with subsequent formation of negative O⁻ or O₂⁻ ions [4,5]. The total induced charge in ionization regime does not depend on the number of electrons attached [3].

The time structure of induced current by a pulsed beam can be obtained with the help of convolution operation of pulse time structure with induced currents (Fig. 2). The nonzero tail at the back front of MGC signal for long beam pulses is caused by the cumulative effect of physical degradation of the counter – Malter effect [6] (see also Fig. 9).

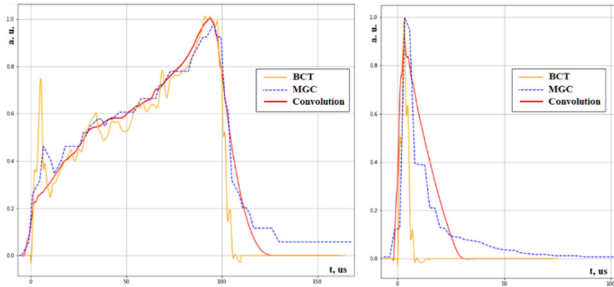


Figure 2: BCT measured signals from a proton macropulse, MGC measured signals from stripes in ionization mode and reconstructed signals with convolution method. Left picture – data for 100 μs beam pulse, right – for 1 μs beam pulse. MGC voltage is 2 kV, the graphs are normalized.

RECOMBINATION MODE

For beam pulses longer than ion collection time charge collection efficiency $f(\xi)$ [7] is:

$$f = \frac{2}{1 + \sqrt{1 + \frac{2}{3} \xi^2}},$$

$$\xi = \frac{md^2\sqrt{q}}{V},$$

where d is electrode spacing, q [C/m³s] is ionization density, m is a constant depending on gas properties, V -applied voltage.

The formula for collection efficiency can fit the experimental saturation curves to find necessary value of m . After it can predict the shape of a signal curve and saturation threshold voltage. It can be done for different values of particles in the beam pulse N_b proportional to q (Fig. 3). The theoretical scaling of saturation voltage comes from the fact that ξ_{sat} is a dimensionless constant and therefore:

$$V_{sat} = const * \sqrt{q}.$$

Or in logarithmic coordinates $V_{sat}(N_b)$ is a line with a slope 0.5 predicted by the theory. The experiment also gives a line, the slope is 0.38 ± 0.01 (Fig. 4).

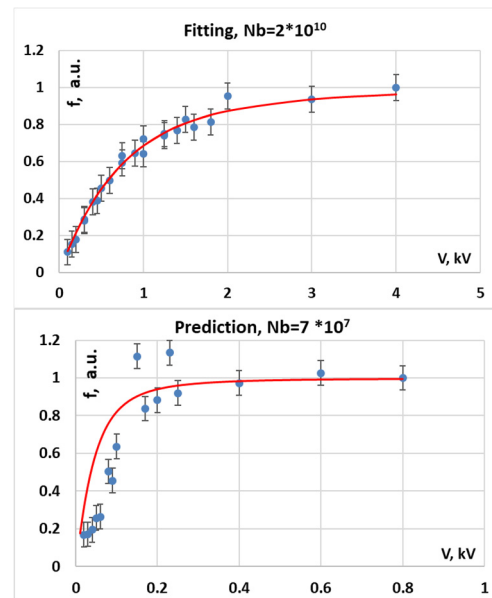


Figure 3: Experimental (blue circles) signal from the ionization chamber and theoretical model (red line). The upper picture is to find parameter m from fitting.

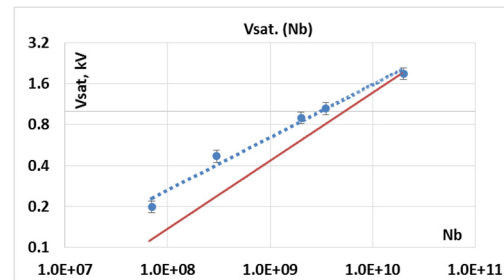


Figure 4: Experimental values (blue dots) and theoretical prediction (red line) of saturation voltage at 0.9 plateau level in a double logarithmic scale.

Another important consequence of the fact that ξ_{sat} is a constant - relation of $V_{sat}(d)$ which helps to find the proper size of a gas gap:

$$V_{sat} = const * d^2.$$

PROPORTIONAL MODE

MGC plates with stripes operate in proportional mode. In this chapter the model to predict gain-voltage properties of a proportional chamber is presented. First the electric field distribution around the stripes was calculated in COMSOL (Fig. 5). The electric field strength along a single line $E(s)$ is of further interest. The result strongly depends on a stripe geometry. This factor mainly defines the error of simulation. Information about detailed stripe shape after etching was needed.

The change in electron (n) and positive ion (m) concentration after passage of ds is:

$$dn = (\alpha - \eta) n ds.$$

$$dm = \alpha n ds,$$

where α and η are townsend ionization and attachment coefficients. A simple integration can be done to get the avalanche plus primary ionization gain. After substitution of $E(s)$, $\alpha(E)$ and $\eta(E)$ in the derived formula one can obtain gain-voltage properties of a proportional chamber (Fig. 6).

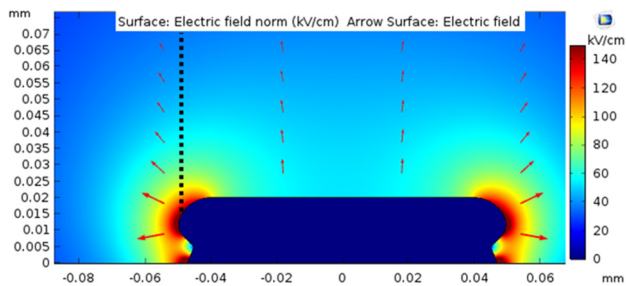


Figure 5: Distribution of electric field near a stripe for 4 kV voltage. The black line is for obtaining $E(s)$.

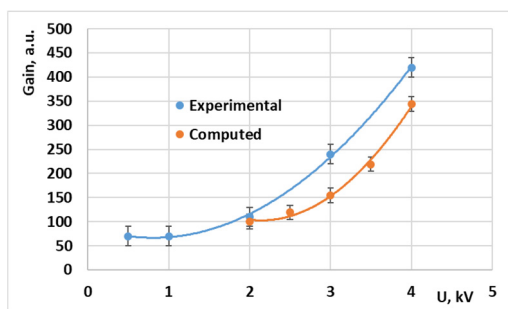


Figure 6: Experimental and computed gain-voltage curves for 94 MeV proton energy for proportional chamber.

MGC EXPLOITATION AND DEGRADATION EFFECTS

The experimental operational range of MGC is 10^7 - 10^{11} p/pulse with pulse duration about 130 μ s. Usage of beams less intensive than 10^7 p/pulse decreases the signal below the sensitivity threshold of MGC electronics.

It was found out, that intensive beams (density $>10^{10}$ p/cm²) lead to oxidation of MGC stripes. Temper colors are visible in Fig. 7.

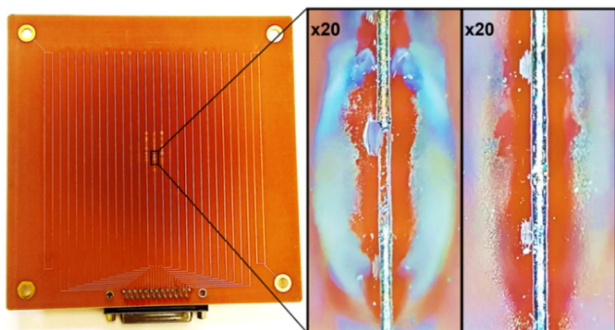


Figure 7: Ageing effects of MGC: stripe destruction and oxidation.

Dielectric oxide film reduces the field strength exerted on particles in avalanche region near stripes and decreases the signal [8]. As an example, profile signal amplitudes in Fig. 8 are almost identical after an irradiation. The way to

solve the problem is to use O₂-free gas filling or measure beam profile without gas amplification. The stripes are subjected to physical degradation and destruction because of high ionization near the electrodes.

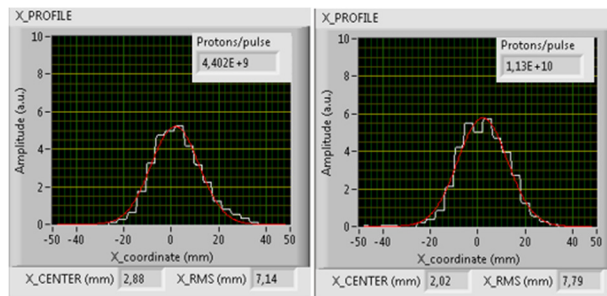


Figure 8: X profiles for a symmetric beam. Left – for $4.4 \cdot 10^9$ protons/pulse; right – after $2.5 \cdot 10^{15}$ protons passed for $1.13 \cdot 10^{10}$ protons/pulse.

Plane chamber electrodes, which are mounted in front of the stripes, are subjected to degradation (Fig. 9). Cathode deposits are also visible. They cause positive charge build-up and electron emission - Malter effect [6].



Figure 9: Photo of plane electrodes of proportional chamber subjected to degradation.

The lower limit for incident beam energy is ~ 20 MeV. Protons with this energy do not reach the last air gap of the counter [2].

NEW DESIGN OF A GAS COUNTER

The new design of MGC consists of only 3 printed-circuit boards instead of 5. The total volume is divided in two parts: segmented ionization chambers, measuring beam current and X, Y profiles in ionization mode. Beam current is obtained by summing the profile signals from stripes in the software.

The material, width, metal coating and active area are the same as in the previous version. One plate with uniform square electrodes on both sides is mounted in the middle of a metal housing and connected to a high voltage terminal (Fig. 10). The remaining two plates have 25 signal stripes with 3.9 mm width and 0.1 mm spacing (Fig. 11). There are also two additional stripes at the edges of the active area at zero potential to form a more homogenous electric field in the active volume. The multichannel plates have a dielectric mask covering to

protect electrical connections. These plates in combination with metal coverings serve as caps to make the total assembly sealed (Fig. 12).

The metal housing has a ring-shaped rubber to prevent a gas leakage. Two screw ports for a gas pumping and pits for electric contacts in the shell of the counter are also visible. The spacing between plates is 8 mm. It was chosen because of mechanical reasons and in order to increase the signal level to compensate partially lack of the gas amplification. The supposed gas filling is N_2 .

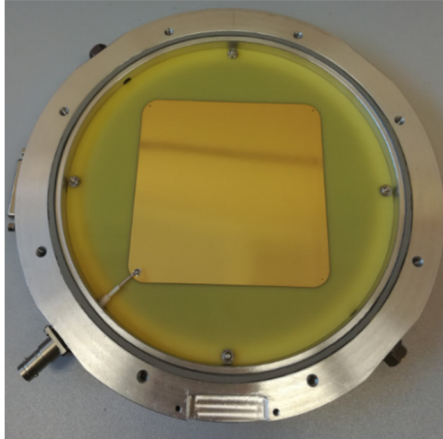


Figure 10: New MGC shell with HV plate.

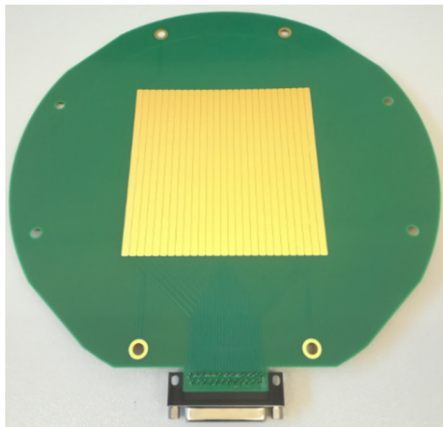


Figure 11: Multichannel plate.

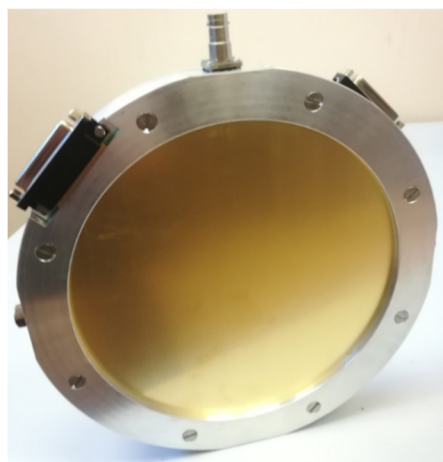


Figure 12: New MGC total assembly.

CONCLUSION

The operational range of MGC was defined during the experiment – $10^7 \div 10^{11}$ p/pulse with pulse duration in range about $50 \div 100 \mu s$. The relative precision of current determination by MGC is about 10%. Analytical models are consistent with experimental data and help to predict the voltage for gas amplification in proportional mode.

The shift of threshold voltage for ionization regime depending on beam current was tested in the experiment and explained. The results show, that the operational voltage of ionization chamber must be set for the beams of highest possible intensity from a working range of a counter. In case of MGC it is 10^{11} protons/pulse and about 2.5 kV threshold voltage. The influence of a gas gap size on the value of saturation voltage of ionization regime is also discussed.

Based on the exploitation experience of MGC, a new device was developed. The new assembly of the detector is sealed and allows to use O_2 -free gas filling to prevent stripe oxidation. The new device works in ionization mode to avoid intense avalanches near thin stripes and their destruction. The gas counter is now thin enough to work in the lower limit of energy range ~ 20 MeV.

REFERENCES

- [1] G. Charpak, F. Sauli, "Multiwire Proportional Chambers and Drift Chambers", CERN, Geneva. Switzerland (1979).
- [2] A. Melnikov, S. Gavrilov, "Multianode Gas Counter For Low Intensity Beam Diagnostics At The INR LINAC", in *Proc. XXVI Russian Particle Accelerator Conference (RuPAC'18)*, Protvino, Russia.
- [3] G. Boissonnat et al., "Measurement of ion and electron drift velocity and electronic attachment in air for ionization chambers", arXiv:1609.03740v1.
- [4] Biagi database, www.lxcat.net, copyright 2010.
- [5] G.J.M. Hagelaar and L.C. Pitchford, "Solving the Boltzmann equation to obtain electron transport coefficients and rate coefficients for fluid models", *Plasma Sci Sources and Tech* 14, 722 (2005).
- [6] J. Va'vra, "Wire Aging", DESY workshop, October 2, 2001.
- [7] J. W. Boag and T. Wilson, "The saturation curve at high ionization intensity", *Br. J. Appl. Phys.* 3, p. 222, 1952.
- [8] T. Z. Kowalski and B. Mindur, "Manifestation of Aging Effect in Gas Proportional Counters", DESY workshop on wire aging, University of Mining and Metallurgy, Cracow, Poland.